33rd Annual International Conference of the IEEE EMBS
Boston, Massachusetts USA, August 30 - September 3, 2011

Estimation of Intraoperative Blood Flow during Liver RF Ablation Using a Finite Element Method-based Biomechanical Simulation

Hiroki Watanabe, Nozomu Yamazaki, Yo Kobayashi, Tomoyuki Miyashita,
Takeshi Ohdaira, Makoto Hashizume, and Masakatsu G. Fujie, *Senior Member*, *IEEE*

Abstract — **Radiofrequency ablation is increasingly being used for liver cancer because it is a minimally invasive treatment method. However, it is difficult for the operators to precisely control the formation of coagulation zones because of the cooling effect of capillary vessels. To overcome this limitation, we have proposed a model-based robotic ablation system using a real-time numerical simulation to analyze temperature distributions in the target organ. This robot can determine the adequate amount of electric power supplied to the organ based on real-time temperature information reflecting the cooling effect provided by the simulator. The objective of this study was to develop a method to estimate the intraoperative rate of blood flow in the target organ to determine temperature distribution. In this paper, we propose a simulation-based method to estimate the rate of blood flow. We also performed an *in vitro* study to validate the proposed method by estimating the rate of blood flow in a hog liver. The experimental results revealed that the proposed method can be used to estimate the rate of blood flow in an organ.**

I. Introduction

Radiofrequency ablation (RFA) is an important method for treating liver tumors, and has seen increasing use in recent years. RFA involves percutaneous introduction of an electrode into the tumor and application of radiofrequency energy, which increases the temperature of the tissue because of ionic agitation generated by the microwaves. Tissue coagulation occurs when the tissue around the electrode reaches a temperature of around 60°C. Moisture evaporation then occurs and the tissue becomes completely necrotic at about 90°C. This percutaneous procedure offers proven effectiveness and safety, and also has the advantage of being minimally invasive.

Manuscript received April 15, 2011. This work was supported in part by the Global COE (Centers of Excellence) Program "Global Robot Academia," in part by "High-Tech Research Center" Project for Private Universities: matching fund subsidy from MEXT (the Ministry of Education, Culture, Sports, Science and Technology of Japan), in part by Grant-in-Aid for Young Scientists (B) (21700513), in part by a Grant for Scientific Research (B) (22360108) from the MEXT, and in part by a Waseda University Grant for Special Research Project (2010B-177).

H. Watanabe, N. Yamazaki, Members of the Graduate School of Science and Engineering, Waseda University, Japan. (59-309, 3-4-1 Okubo, Shinjuku Ward, Tokyo, Japan, e-mail: hiroki_watanabe@suou.waseda.jp, tel: +81-3-5286-3412, fax: +81-3-5291-8269).

Y. Kobayashi, T. Miyashita, M. G. Fujie, Members of the Faculty of Science and Engineering, Graduate School of Science and Engineering, Waseda University, Japan.

M. Hashizume, Member of the Center for the Integration of Advanced Medicine and Innovative Technology, Kyushu University Hospital, Japan.

A. Practical limitations of RFA

Although RFA is a minimally invasive procedure, it does have some limitations, such as: 1) imaging modalities such as ultrasonography can only display a monochromatic image of the ablation area; 2) the power supply is not optimized for the formation of an adequate ablation area; and 3) it is not possible to generate an adequate ablation area for large tumors because of the cooling effect of capillary vessels. These limitations mean it is difficult to precisely control the formation of the coagulation zones, which may allow tumors to recur in areas that have not been fully cauterized.

B. Robot-assisted RFA

In recent years, considerable research has been undertaken to develop surgical robots and navigation systems for minimally invasive and precise surgery [1]-[3]. We have also proposed a robot-assisted RFA therapeutic system (Fig. 1) [4]–[7]. This robotic system is based on a thermophysical model of the organ, which predicts the temperature distribution of the organ during RFA in real time to calculate and supply the adequate amount of electrical power to the RF electrode for precise intraoperative surgical control.

C. Thermophysical model of organs

The thermophysical model of an organ, such as the liver, is constructed from two essential components, the first being a database of the thermophysical properties of the organ, which includes data such as specific heat, thermal conductivity and the rate of blood flow. The other is an accurate temperature distribution simulator developed using the finite element method (FEM). An accurate simulator requires the thermophysical properties of the organ. However, creating an accurate thermophysical model is a challenge, given the complex thermophysical properties of organs.

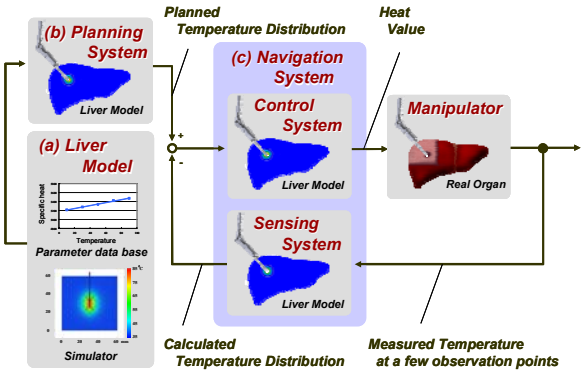

Fig. 1. Robot-assisted RFA therapy.

There are two complexities of the thermophysical properties of the organ.

The first is that the specific heat and thermal conductivity, essential thermophysical properties of the organ, change according to tissue temperature during RFA. It is possible that these two properties change significantly because of protein denaturation as tissue temperature rises. In fact, Webster et al. and Wolf et al. indicated that there is a possibility that the tissue temperature dependence of the thermophysical properties affects the accuracy of temperature distribution simulators for RFA [8], [9]. However, those studies did not describe whether these temperature-dependent properties affect the results of simulations in quantitative experiments. We have already measured and reported the temperature dependence of specific heat and thermal conductivity of the liver in experiments. In addition, we have validated the effect of the temperature dependence of liver on the spatial and temporal tissue temperature changes during RFA [10], [11].

The other complexity is that the temperature at the affected area does not increase to the temperature required for coagulation regions with extensive capillary blood flow [12]-[16]. Indeed, it is accepted that the size of the coagulated area varies according to the rate of blood flow in capillary vessels in the target area because the heat generated by the RF needle is absorbed by the capillary vessels. This phenomenon is called the cooling effect. It is also known that the amount of heat absorbed by the capillary vessels is affected by the physiological state of patient and the surgical procedure because the rate of blood flow is significantly different due to the physiological state of patient and surgical situation.

The novelty of our work lies in the development of a temperature distribution simulator to predict the temperature change during RFA reflecting the cooling effect of capillary vessels estimating the intraoperative rate of blood flow in the target organ. We propose a novel method to estimate the rate of blood flow in the liver in real time during RFA. This method decides the rate of blood flow intra-operatively by comparing the simulated temperature change of RF needle and measured temperature change of RF needle during RFA. The objective of this paper is to investigate the concept of our method with preliminary *in vitro* experiments.

This report is organized as follows: Section II provides a detailed description of the method used to estimate the rate of blood flow in an organ during RFA. Section III describes the simulation used to estimate the rate of blood flow of the liver. Section IV presents the *in vitro* experiment performed to validate the estimation method using hog liver as an experimental model. Finally, section V presents our conclusions and plans for future work .

II. METHOD TO ESTIMATE THE RATE OF BLOOD FLOW

In general, the tissue temperature distribution during RFA can be simulated using Pennes bio-heat Eq. (1) [17].

$$\rho c \frac{\partial T}{\partial t} = \lambda \nabla^2 T + \sigma |E|^2 - \rho \rho_b c_b F (T - T_b) + Q_m \qquad (1)$$

where ρ is the density of the organ [kg/m^3], c is its heat capacity [J/kgK], T is its temperature [°C], λ is its thermal conductivity [W/mK], σ is its electrical conductivity [S/m], E is its electrical field [V/m], ρ_b is the density of blood, c_b is the heat capacity of blood, F is the rate of blood flow of the organ [m^3/kgs], T_b is the blood temperature, Q_m is the metabolic heat source of the organ [W/m^3].

In Eq. (1), the absorption of heat by the capillary vessels is described by the third term on the right hand side. To simulate the tissue temperature distribution reflecting the intraoperative cooling effect, it is necessary to determine the rate of blood flow F during RFA in real time. It is also necessary to assign the obtained value to the third term on the right hand side and hence solve Eq. (1) for temperature T. In this research, we propose a method to estimate F by applying the phenomenon that the rate of increase in temperature of the RF needle is correlated with F when inputting the step wave of constant heat into the tissue by the needle. This phenomenon is also used as the experimental principle of the unsteady hot wire method to measure the thermal conductivity of any material. The specific procedure used to estimate the rate of blood flow is described below.

1) Estimation of the correlation between the rate of blood flow and the rate of increase in temperature of the RF needle. First, we determined the correlation between the rate of blood flow and the rate of increase in temperature of the RF needle when transferring the step wave of heat into the organ using a simulation. Based on the FEM, the rate of change in temperature of the needle is numerically calculated using Eq. (1) while changing the rate of blood flow in Eq. (1).

2) Measurement of the actual increase in temperature of the RF needle during RFA. Next, the actual rate of increase in temperature of the RF needle is measured intraoperatively using the RF needle's thermocouple, when transferring the step wave of constant heat into the organ.

3) Determination of the actual rate of blood flow in the organ: Finally, the actual rate of blood flow was determined so that the measured increase in temperature is equal to the simulated increase in temperature. This means that parameter F in the simulation model is determined in a reverse manner so that the measured rate of increase in temperature of the needle matches that determined by the simulation.

III. SIMULATION

In this section, we describe the simulation used to determine the correlation between the rate of blood flow and the rate of increase in temperature of the RF needle during liver RFA. Using the FEM, this correlation was determined by calculating the temporal change in temperature of the needle while changing the value of F within a physiological range. In this simulation, the target organ was the liver and a step wave with a constant amount of heat was assumed to be transferred into the liver by the needle.

A two-dimensional temperature distribution simulation based on the FEM Eq. (2), which was derived from Pennes bio-heat Eq. (1), was used in this simulation.

$$[C]\frac{\partial\{T\}}{\partial t}+[K]\{T\}=\{Q\} \quad (2)$$

Where $\{T\}$ is the temperature vector, $[C]$ is the heat capacity matrix, including the specific heat of the liver, $[K]$ is the heat conductivity matrix, including the thermal conductivity of the liver, and $\{Q\}$ is a heat flux vector incorporating the heat flow supplied by the needle and that absorbed by capillary blood vessels, including the rate of blood flow F.

A. Simulation conditions

Fig. 2 shows the liver model used for the simulation. The model used a 70 mm × 70 mm square shape. The needle was considered to be inserted from the top surface of the liver into the center of the model. The model comprised 2144 and 1168 elements and nodes, respectively. The amount of step wave heat supplied to the liver by the needle was 15.6 W/m, which matched the *in vitro* validation experiment described in section IV. The initial thermal condition of 20°C was applied for all elements, and the thermal boundary condition for the surface of the square was 20°C. The temperature of the capillary vessel was kept at 19°C. These temperatures matched those of the *in vitro* validation experiment described in section IV.

TABLE I
THERMAL PROPERTIES USED IN THE SIMULATION

Density ρ_{Liver} kg/m^3	1060
Specific heat c_{Liver} J/kgK	$3.2T_{Liver}+3.2\times10^3$
Thermal conductivity λ_{Liver} W/mK	$3.0\times10^{-4}T_{Liver}+5.2\times10^{-1}$ ($0\le T_{Liver}\le70$) $2.1\exp(-2.0\times10^{-2}T_{Liver})$ ($70<T_{Liver}$)
Density ρ_{Blood} kg/m^3	1000
Specific heat c_{Blood} J/kgK	4180
Heat quantity Q_{needle} W/m	15.6
Blood perfusion F m3/kgs	0–15.0

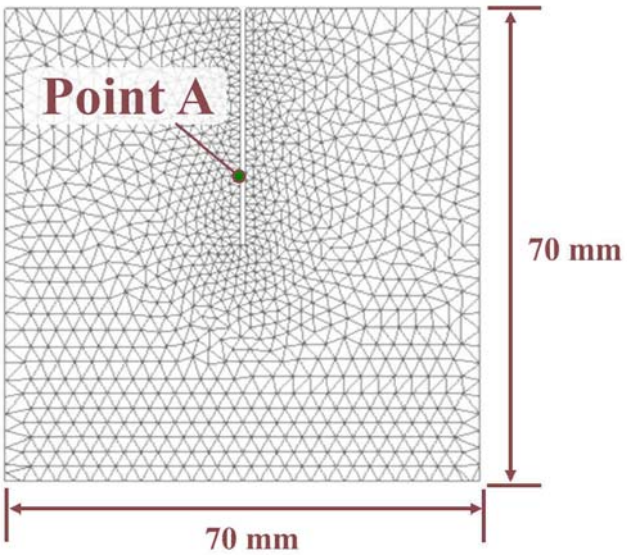

Fig. 2. Analytical liver model.

B. Thermophysical properties

Table I shows the thermophysical properties used in the simulation. The density of the liver ρ_{Liver}, the density of capillary vessels ρ_{blood} and the specific heat of capillary vessels c_{blood} were determined based on the work by Duck [17] and Tungjitkusolmun [18]. The effective specific heat of the liver c_{Liver} and the effective thermal conductivity of the liver λ_{Liver} were the temperature-dependent values obtained in our previous work using isolated hog liver without blood flow [10],[11]. We repeated the simulation by changing F from 0 to 21.7×10^{-6} m^3/kgs at intervals of 1.70×10^{-6} m^3/kgs. The minimum value of 0 m^3/kgs represents the absence of blood flow *in vitro* while the maximum value of 21.7×10^{-6} m^3/kgs represents the theoretical maximum value of liver RFA.

C. Simulation results

Figs. 3 and 4 show the simulated temperature distributions at 5.0 s and 30.0 s when F is 0 and 21.7×10^{-6} as representative examples of the simulation. These two figures show that the heated area was confined to the immediate vicinity of the needle. Fig. 5 shows the temporal change in temperature on the surface of the needle at point A and that the temperature at this point increases logarithmically over time for all rates of blood flow. The rate of increases in temperature also gradually decreases as the rate of blood flow is increased. The correlation between the rate of blood flow and the logarithmic rate of increase in temperature is shown in Fig. 6. This figure shows that the logarithmic rate of increase in temperature $\Delta T/\Delta\ln t$ decreases exponentially as F increases. This relationship can be described using Eq. (3).

$$\frac{\Delta T}{\Delta\ln t}=ae^{bF} \quad (3)$$

Where a is 1.99 [K] and b is -3.68×10^4 [1/s].

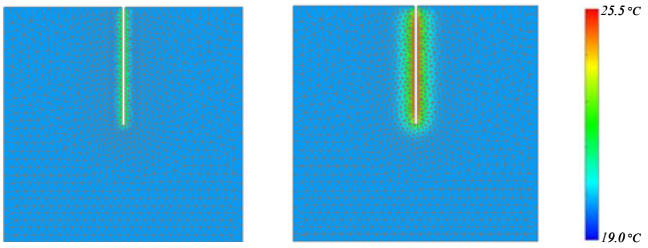

(a) 5.0 s (b) 30.0 s

Fig. 3. Simulation result at $F=0$ m^3/kgs.

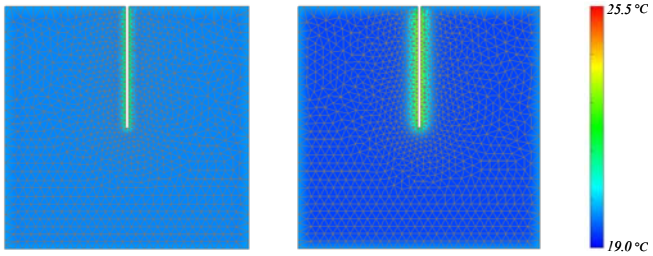

(a) 5.0 sec (b) 30.0 sec

Fig. 4. Simulation result at $F=21.7\times10^{-6}$ m^3/kgs.

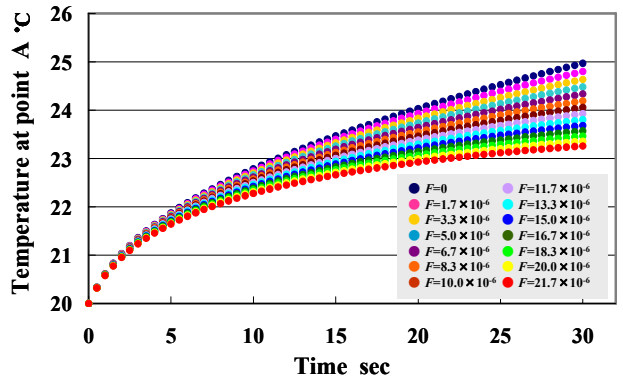

Fig. 5. Temporal change in temperature at point A.

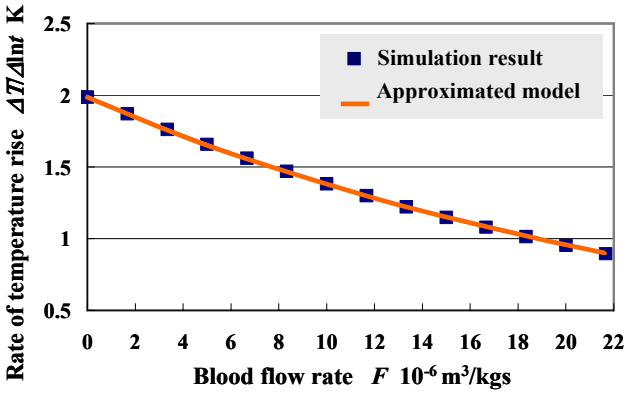

Fig. 6. Relation between the rate of blood flow and the temperature rise.

IV. In Vitro Experiment

Next, we carried out an *in vitro* experiment to estimate the rate of blood flow in a hog liver to validate our method.

A. Method

Fig. 7 shows the experimental setup. We supplied water instead of blood to the inferior vena cava of the isolated hog liver via a tube connected to a water pump to mimic blood flow in the liver *in vivo*. Then, the step wave of constant heat was transferred via a needle inserted into the hog liver using a heating device. The rate of blood flow of the hog liver was determined by referring to the measured rate of increase in temperature of the needle and the derived correlation between the rate of blood flow and the rate of increase in needle temperature shown in Eq. (3). The temperature of the liver and water were 20°C and 19°C, respectively, as used in the simulation described in Section III. We believe it is unlikely that differences in the shape or size of the liver between the simulation and the experiment will affect the temperature of the needle. This is because the heating area was limited to the immediate vicinity of the needle and the boundary condition did not affect the temperature around the needle. In addition, the needle used in this experiment included a thin wire to generate the heat and a thermocouple to measure the temperature of the needle. The current I = 0.625 A flowed through the thin wire with a resistance R = 25.0 Ω/m. As a result, the heat output Q = 15.6 W/m ($=I^2R$) was generated and transferred into the liver. This heat value was the same as that used in the simulation in section III.

We also estimated the rate of blood flow under the condition that water was not pumped into the liver to determine the difference in the estimated rate of blood flow between the presence and absence of water flow. The experiments were performed at different two points, A and B, to compare the estimated rates of blood flow between different areas of the liver (Fig. 8). Therefore, four conditions were used, as follows:

(a) Point A without water flow.
(b) Point A with water flow.
(c) Point B without water flow.
(d) Point B with water flow.

We carried out two trials in each condition using a hog liver.

B. Results

Table II shows the experimental results obtained from both trials in all four conditions. Fig. 9 shows the estimated rate of blood flow of the hog liver. Based on Fig. 9, the experimental results can be summarized as follows. First, the rate of blood flow at points A and B in the absence of water flow is almost 0. In the presence of water flow, the rate of blood flow at point A was about 1.8 times greater than that at point B.

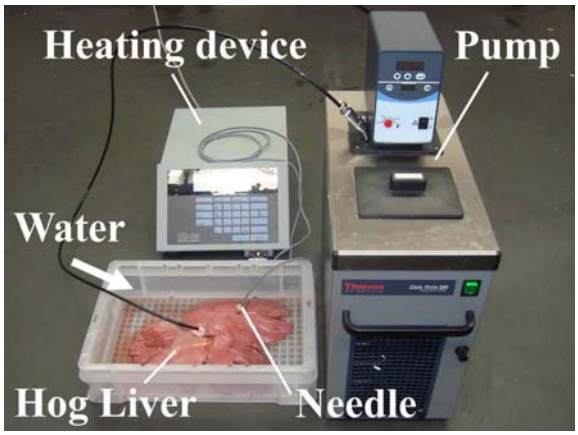

Fig. 7. *In vitro* experimental setup.

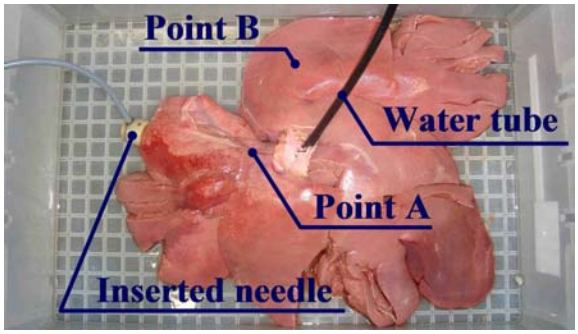

Fig. 8. Isolated hog liver used in the experiment.

TABLE II
RATE OF INCREASE IN TEMPERATURE OF THE NEEDLE $\Delta T/\Delta \ln t$

	Condition (a)	Condition (b)	Condition (c)	Condition (d)
Trial 1	1.989	1.341	1.977	1.566
Trial 2	1.985	1.410	1.965	1.586
Mean	1.987	1.375	1.971	1.576

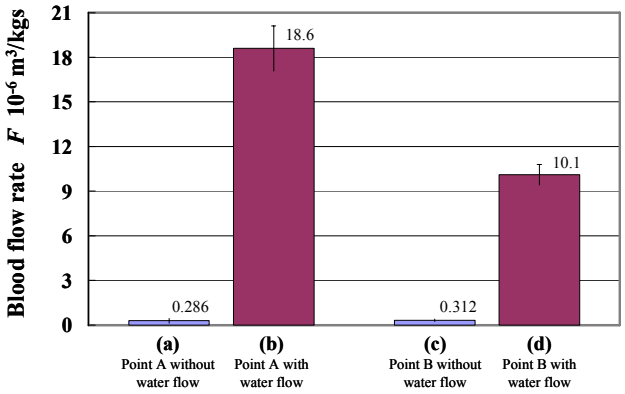

Fig. 9. Estimated rates of blood flow in a hog liver.

C. Discussion

In this experiment, all of the estimated rates of blood flow determined in conditions (a) to (d) were within the expected ranges for the liver. This suggests that the rates of blood flow estimated by our method are reasonable and consistent with those of physiological tissue. We suspect that the higher rate of blood flow at point A was due to the greater number of capillary vessels neighboring point A compared with that at point B, because point A is closer to the inferior vena cava than is point B.

These experimental results support the feasibility of the proposed intraoperative method to estimate the rate of blood flow. In the future, we will need to carry out detailed experiments to validate the accuracy of our proposed method by measuring the rate of blood flow using laser blood flow meters or electromagnetic blood flow meter. Moreover, we need to validate the proposed method *in vivo*.

V. Conclusion and Future Work

This paper presented a method to estimate the rate of blood flow in an organ intraoperatively using a FEM-based simulation. This method simulates the temperature distribution associated with the cooling effect to help plan and control the electric power supplied to a RF needle for robotic RFA. First, we described a method that can be used to estimate the rate of blood flow. Next, we determined the correlation between the rate of blood flow and the rate of increase in temperature of the RF needle when the step wave of heat was transferred into the target organ (liver) using the RF needle. Finally, we performed *in vitro* experiments to estimate the actual rate of blood flow in a hog liver to which we supplied water instead of real blood. The results of the experiment support the feasibility of the proposed method to estimate the intraoperative rate of blood flow in an organ.

In the future, *in vitro* and *in vivo* experiments will be needed to validate the accuracy of the rate of blood flow estimated using this method. Moreover, a method to control the amount of electric power supplied to the needle will need to be developed. The amount of electric power is determined based on the real-time temperature distribution around the affected area. The information is provided in real time by a numerical simulator, which also estimates the rate of blood flow at the affected area using the proposed method. Using this method, it will be possible to determine the appropriate coagulation area, even if the affected area receives much blood flow during RFA.

References

[1] R. H. Taylor, D. Stoianovici, "Medical robotics in computer-integrated surgery", *IEEE Trans. Robot. Autom.,* vol. 19, no. 5, pp. 765–781, 2003.

[2] P. Dario, B. Hannaford, and A. Menciassi, "Smart surgical tools and augmenting devices", *IEEE Trans. Robot. Autom.,* vol. 19, no. 5, pp. 782–792, 2003.

[3] P. Kazanzides, G. Fichtinger, G. D. Hager, A. M. Okamura, L. L. Whitcomb, R. H. Taylor, "Surgical and Interventional Robotics", *IEEE Robotics & Automation Magazine,*vol. 15, pp. 122-130, 2008.

[4] Y. Kobayashi, J. Okamoto, and M. G. Fujie, "Physical properties of the liver for needle insertion control", *IEEE Int. Conf. Intell. Robot. Syst.,* pp. 2960–2966, 2004.

[5] Y. Kobayashi, J. Okamoto, M. G. Fujie, "Physical properties of the liver and the development of an intelligent manipulator for needle insertion", *IEEE Int. Conf. Robot. Autom.,* pp. 1644–1651, 2005.

[6] Y. Kobaysshi, A.Onishi, H. Watanabe,T. Hoshi, K. Kawamura, M. G. Fujie, "Developing a planning method for straight needle insertion using probability-based condition where a puncture occurs", *IEEE Int. Conf. Robot. Autom.,* pp. 3482–3489, 2005.

[7] H. Watanabe, Y. Kobayashi, M. G. Fujie, "Modeling the temperature dependence of thermal conductivity: developing a system for robot-assisted RFA therapy", *Proc. 2nd IEEE/RAS-EMBS Int. Conf. Biomed. Robot. Biomechatronics*, pp. 483–488, 2008.

[8] J. G. Webster, *et al.*, "Finite-element analysis of hepatic multiple probe radio-frequency ablation", *IEEE Trans. Biomed. Engin.,* vol. 49, no. 7, pp. 836–842, 2002.

[9] P. D. Wolf, *et al.*, "A three-dimensional finite element model of radiofrequency ablation with blood flow and its experimental validation", *Ann. Biomed. Engin.,* vol. 28, pp. 1075–1084, 2000.

[10] H. Watanabe, Y. Kobayashi, M. G. Fujie, "Modeling the temperature dependence of thermo physical properties: study on the effect of temperature dependence for RFA", in *Proc. 31st Ann. Int. Conf. IEEE Engin. Med. Biol. Soc.,* pp. 5100-5105, 2009.

[11] H. Watanabe, N. Yamazaki, Y. Kobayashi, T. Miyashita, M. Hashizume, M. G. Fujie, "Temperature dependence of thermal conductivity of liver based on various experiments and a numerical simulation for RF ablation", in *Proc. 32nd Ann. Int. Conf. IEEE Engin. Med. Biol. Soc.,* pp. 3222–3228, 2010.

[12] R. J. Podhajsky, M. Yi, R. L. Mahajan, "Differential and Directional Effects of Perfusion on Electrical and Thermal Conductivities in Liver", in *Proc. 31st Ann. Int. Conf. IEEE Engin. Med. Biol. Soc.,* pp. 4295–4298, 2009.

[13] D. Haemmerich, "Hepatic radiofrequency ablation -An overview from an engineering perspective", in *Proc. 26th Ann. Int. Conf. IEEE Engin. Med. Biol. Soc.,* pp. 5433-5436, 2004.

[14] J. D. Brannan, C. M. Ladtkow, "Modeling Bimodal Vessel Effects on Radio and Microwave Frequency Ablation Zones", in *Proc. 31st Ann. Int. Conf. IEEE Engin. Med. Biol. Soc.,* pp. 5989–5992, 2009.

[15] D. Haemmerich, D. J. Schutt", *IEEE Trans. Biomed. Engin.,* vol. 58, no. 2, pp. 404–410, 2011.

[16] S. Tungjitkusolmun, J. G. Webster, *et al.*, "Guidelines for Predicting Lesion Size at Common Endocardial Locations During Radio-Frequency Ablation", *IEEE Trans. Biomed. Engin.,* vol. 48, no. 2, pp. 194–201, 2001.

[17] H. H. Pennes, "Analysis of tissue and arterial blood temperatures in the resting human forearm", *J. Appl. Physiol.,* vol. 1, no. 2, pp. 93–122, 1948.

[18] F. Duck, *Physical Properties of Tissue*, New York, NY: Academic Press, pp. 167–223,1990.

[19] S. Tungjitkusolmun, *et al.*, "Three-dimensional finite-element analysis for radio-frequency hepatic tumor ablation", *IEEE Trans. Biomed. Engin.,* vol. 49, no. 1, pp. 3–9, 2002.